

Stable chemical bonding of porous membranes and poly(dimethylsiloxane) devices for long-term cell culture

Christopher G. Sip and A. Folch

Citation: *Biomicrofluidics* **8**, 036504 (2014); doi: 10.1063/1.4883075

View online: <http://dx.doi.org/10.1063/1.4883075>

View Table of Contents: <http://scitation.aip.org/content/aip/journal/bmf/8/3?ver=pdfcov>

Published by the [AIP Publishing](#)

Articles you may be interested in

[Single cell kinase signaling assay using pinched flow coupled droplet microfluidics](#)
Biomicrofluidics **8**, 034104 (2014); 10.1063/1.4878635

[A novel surface modification technique for forming porous polymer monoliths in poly\(dimethylsiloxane\)](#)
Biomicrofluidics **6**, 016506 (2012); 10.1063/1.3693589

[Electrophoretic separation of neurotransmitters on a polystyrene nano-sphere/polystyrene sulphonate coated poly\(dimethylsiloxane\) microchannel](#)
Biomicrofluidics **5**, 034104 (2011); 10.1063/1.3609968

[Systematic characterization of degas-driven flow for poly\(dimethylsiloxane\) microfluidic devices](#)
Biomicrofluidics **5**, 024108 (2011); 10.1063/1.3584003

[Thermomodulated cell culture/harvest in polydimethylsiloxane microchannels with poly\(N-isopropylacrylamide\)-grafted surface](#)
Biomicrofluidics **4**, 044107 (2010); 10.1063/1.3516038



Re-register for Table of Content Alerts

Create a profile.



Sign up today!



Stable chemical bonding of porous membranes and poly(dimethylsiloxane) devices for long-term cell culture

Christopher G. Sip^{a)} and A. Folch

Department of Bioengineering, University of Washington, Seattle, Washington 98185, USA

(Received 18 February 2014; accepted 2 June 2014; published online 16 June 2014)

We have investigated the bonding stability of various silane treatments for the integration of track-etched membranes with poly(dimethylsiloxane) (PDMS) microfluidic devices. We compare various treatments using trialkoxysilanes or dipodal silanes to determine the effect of the organofunctional group, cross-link density, reaction solvent, and catalyst on the bond stability. We find that devices made using existing silane methods delaminated after one day when immersed in cell culture medium at 37 °C. In contrast, the dipodal silane, bis[3-(trimethoxysilyl)propyl]amine, is shown to yield stable and functional integration of membranes with PDMS that is suitable for long-term cell culture. To demonstrate application of the technique, we fabricated an open-surface device in which cells cultured on a track-etched membrane can be stimulated at their basal side via embedded microfluidic channels. C2C12 mouse myoblasts were differentiated into myotubes over the course of two weeks on these devices to demonstrate biocompatibility. Finally, devices were imaged during the basal-side delivery of a fluorescent stain to validate the membrane operation and long-term stability of the bonding technique. © 2014 AIP Publishing LLC.

[<http://dx.doi.org/10.1063/1.4883075>]

INTRODUCTION

The integration of commercially available track-etched membranes in microfluidic devices has experienced growing interest because these materials offer well-defined nano- or micro-pore structures in a monolithic material.^{1–3} Poly(ethylene terephthalate) (PET) track-etched membranes are available in a transparent format that is especially useful for microscopy and live-cell observation. A variety of cell-based devices have been designed to spatially control delivery of reagents to cells, e.g., to apply gradients for chemotaxis,^{3–5} control differentiation,^{6,7} compartmentalize cell co-cultures,^{8,9} and organs-on-chips.¹⁰ Across these studies, a variety of techniques have been reported for integrating track-etched membranes with microfluidic layers. Techniques include sandwiching between plasma bonded poly(dimethylsiloxane) (PDMS) layers,^{4,11–13} using adhesives,^{14–16} PDMS gluing,^{8,17,18} SiO₂ sputtering,^{6,19} and silane coupling.^{8,20}

Silane coupling is an attractive technique because the process uses commercially available reagents, works well with polymers whose surfaces can be hydroxylated, is uniformly applied to surfaces (thus tends to be feature-independent), and is compatible with familiar oxygen plasma-bonding steps. In contrast to the sandwiching technique,^{4,11–13} silane coupling permits open-surface devices through bonding of only one side of a membrane. Furthermore, PDMS gluing and the use of adhesives pose limitations on feature-size due to problems with leakage or contamination of high-resolution structures. SiO₂ sputtering relies on expensive and specialized equipment that limits its widespread use. Silane coupling has an extensive history for the coupling of dissimilar materials²¹ and several groups have reported on methods using (3-Aminopropyl)-triethoxysilane (APTES) modification of plastics to achieve bonding with PDMS.^{22–24} Similarly, Lee and Ram demonstrated the enhanced stability of plastic-PDMS

^{a)}Author to whom correspondence should be addressed. Electronic mail: csiprun@u.washington.edu.

bonding using thick layers of dipodal silane,²⁵ however, this method is unsuitable for porous membranes due to occlusion of the pores. The Zahn group first reported the modification of porous polymer membranes with APTES for integration with PDMS device layers.²⁰ Encouraged by these reports, we evaluated bonding methods for the fabrication of cell culture devices incorporating porous membranes having an open-surface (where the membrane is exposed to the surrounding medium and available as a substrate for cell culture). For these devices, we found that APTES modification yields immediate bond formation and stability when stored in water; however, rapid bond degradation occurs when immersed in a common cell culture medium. The enhanced bond failure in cell culture medium can be attributed to the high concentration of salt cations having a catalytic effect on the dissociation of Si-O bonds within the silane interface.²⁶ Additionally, we propose that the observed increased rate of delamination is due to the high porosity of the membrane and open-surface configuration of the devices.

To find a solution, we tested a variety of silane preparations for their ability to bond PET track-etched membranes and PDMS in an open-surface configuration. We tested formulations of several trialkoxysilanes and dipodal silanes to determine a combination of organofunctional group, cross-link density, solvent, and catalyst conditions for long-term bond stability in cell culture medium. From this testing, we have found a robust silane modification process and applied this to demonstrate unique functionality of integrated track-etched membranes and PDMS devices for cell culture.

EXPERIMENTAL

Materials

The silanes bis[3-(trimethoxysilyl)propyl]amine (bis-amino silane), (3-Aminopropyl) triethoxy-silane (APTES), (3-Glycidyloxypropyl)-trimethoxysilane (epoxy silane), and tetrabutyl titanate (TBT) and diisopropylamine were purchased from Sigma-Aldrich (St. Louis, MO). Transparent PET track-etched membranes with $0.4\text{ }\mu\text{m}$ pore diameter and 2×10^6 pores cm^{-2} in either 13 mm or 25 mm diameters were purchased from AR Brown-US (Pittsburgh, PA). Dulbecco's Modified Eagle Medium (DMEM) cell culture medium (11995), fetal bovine serum (10082), penicillin-streptomycin (10378016), Hank's balanced salt solution (HBSS, 14025), and calcein AM (C3100MP) were obtained from Life Technologies (Grand Island, NY). Matrigel (356234) was purchased from BD Biosciences (San Jose, CA).

Silane treatment of PET track-etched membranes

We assayed various silane formulations in order to determine their effectiveness for bonding PET membranes with PDMS. In general, membranes were secured by their edge using a PDMS block and positioned upright when treated with oxygen plasma for 60 s at 60 W, 670 mTorr, and 40 kHz (Zepto plasma system, Diener Electronic, Germany). After plasma oxidation membranes were then submerged in prepared silane mixtures for 20 min at 80 °C on a hotplate. After treatment with silane, the membranes were rinsed with copious IPA and cured for 30 min at 70 °C in a convection oven. Membranes were then immersed in 70% ethanol for 30 min to render the surface hydrophilic. PDMS slabs were treated with oxygen plasma then bonded to membranes by conformal contact, so that the membranes are bonded to PDMS on only one side. Bonded pieces were then allowed to cure for 1 h at 70 °C. A generalized reaction scheme for the optimal bonding strategy with 2% bis-amino silane and 1% water in IPA is shown in Fig. 1. To evaluate bond stability, bonded PDMS-PET samples were prepared in quadruplicates for each silane formulation and submerged in DMEM at 37 °C. Delamination was observed after one day and two weeks of immersion. A qualitative score was assigned (see Table I) by grasping the membrane with tweezers and gently lifting the sample out of the DMEM medium, so that detachment could be observed while applying minimal force to the bond interface.

X-ray photoelectron spectroscopy (XPS)

Samples of untreated, oxygen plasma treated, freshly silane-modified, and degraded silane-modified membranes were analyzed with XPS (Kratos Axis Ultra DLD, Kratos Analytical, Inc.,

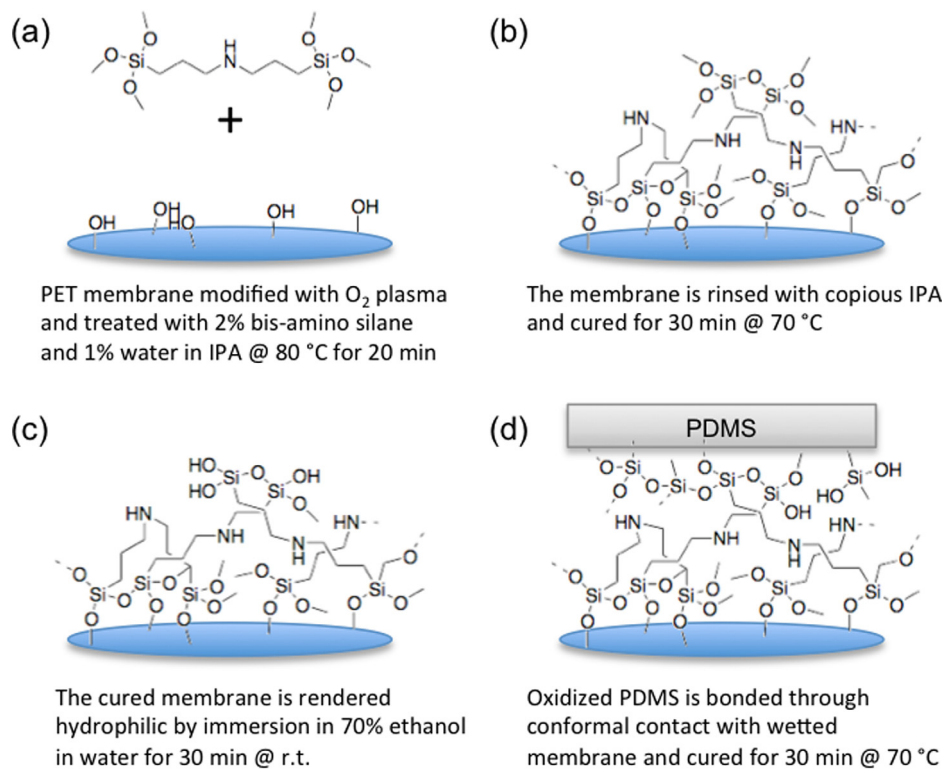


FIG. 1. The bis-amino surface modification process and bonding reaction for PET membranes. (a) An oxidized PET membrane is a substrate for the condensation of bis-amino silane at elevated temperature. (b) After the condensation reaction, residual unbound silane is rinsed and the substrate is cured in order to further cross-link the silane layer. (c) The modified membrane is submerged in a 70% ethanol in water solution to hydrate the surface and expose hydroxyl groups. (d) Oxidized PDMS bonds readily to the wetted membrane. Complete bonding occurs when the surface is dried and baked.

NY) to determine the average elemental compositions. Three spots of $700 \times 300 \mu\text{m}^2$ area per sample were analyzed with survey scans to quantify the C 1s and O 1s peaks at a resolution of 1 eV. Detailed scans were used for analysis of the N 1s and Si 2p spectra at a resolution of 0.3 eV. Samples were analyzed at an angle of 0° with respect to the normal of the surface.

Photoelectrons were detected from a depth of approximately 10 nm. Silane modification of membranes with 2% bis-amino, 1% water, in IPA or 2% APTES in water was done as previously described. For freshly prepared samples, membranes were modified with silane, dried,

TABLE I. Comparison of APTES and bis-amino silanes.

No.	Solvent	Silane	Catalyst	Bond ^a	DMEM 1 day	DMEM 2 weeks
1	Water	APTES	100% water	2	0	...
2	Water	bis-amino	100% water	2	0	...
3	Water	APTES or epoxy	100% water	2	0	...
4	IPA	APTES	1% water	2	0	...
5	IPA	bis-amino	1% water	2	2	2
6	IPA	APTES	0.5% TBT	2	0	...
7	IPA	bis-amino	0.5% TBT	2	2	1
8	IPA	APTES	none	2	0	...
9	IPA	bis-amino	none	2	2	1
10	IPA	APTES or epoxy	0.5% TBT	2	2	2
11	IPA	1:1 bis-amino with APTES or epoxy	0.5% TBT	2	2	0

^aBond score: 2: bonded, 1: partial bond failure, 0: total bond failure.

and then analyzed with XPS. For degraded silane-modified samples, membranes were modified then submerged in water, HBSS, or DMEM for 18.5 h before rinsing, drying, and analysis with XPS.

Fabrication of a PDMS-PET membrane device for basal-side stimulation of cell cultures

For proof-of-concept, we designed a simple open-surface PDMS-PET membrane device for the basal-side stimulation of cell cultures. In order to achieve high quality imaging of cells, the device was fabricated using 400 μ m thick PDMS replicas that were micromolded from SU-8 patterned silicon masters by exclusion molding technique.²⁷ The PDMS replicas were plasma-bonded to cover glass-bottom 55 mm dishes (No. 60-30-1-N, *In Vitro* Scientific, Sunnyvale, CA) to produce a self-contained cell culture format. Plasma-oxidized track-etched PET membranes were treated with 2% bis-amino silane in 1% water and IPA as previously described. After treatment, curing, and soaking in 70% ethanol and water solution, the silane-modified membranes were brought into conformal contact with the device consisting of the PDMS replica and 55 mm dish. Bonding while the membranes are slightly wetted with 70% ethanol solution enhances wrinkle-free assembly. After drying with an air gun, the assembly was baked for 30 min at 70 °C to complete the bonding. Vias were produced by cutting and removing the membrane with dissection tweezers at the location of the inlets and outlets of the underlying microchannels. Finally, inlet and outlet ports comprised of PDMS slabs were plasma bonded to complete the devices.

C2C12 cell culture and calcein AM stimulation

Assembled PDMS-PET membrane devices were coated with a 1:50 dilution of Matrigel for 30 min at 37 °C. C2C12 myoblasts (American Type Culture Collection, Manassas, VA) were uniformly seeded onto the coated devices and maintained in DMEM with 20% fetal bovine serum and 1% penicillin-streptomycin until they achieved confluence after approximately 1 week in culture. “Serum starvation” (changing the serum conditions to 2% horse serum) induced myotube differentiation over the course of an additional week of culture.²⁸ Calcein AM was prepared in Hank’s balanced salt solution at 0.5 μ M concentration and loaded into cells through the microchannels for 15 min before imaging.

RESULTS AND DISCUSSION

Evaluation of different silane treatments for bond stability in DMEM at 37 °C

In order to determine an effective strategy for bonding PET membranes with PDMS, we assayed different formulations of 2% silane in quadruplicates while varying the following parameters of the silane formulations: (1) trialkoxy- or dipodal silanes, (2) catalyst, (3) organo-functional group, and (4) reaction solvent. We tested formulations using APTES and the dipodal silane bis[3-(trimethoxysilyl)propyl]amine (referred to herein as bis-amino silane) with polar protic solvents and different catalysts. Bond stability was assessed with a scoring system such that a result of “0” meant membranes were found to be completely detached from the PDMS, “1” partially detached, or “2” fully bonded. The scores for quadruplicates of each condition showed no deviation. In Table I, for treatments 1–3, we used 100% water as choice of solvent and catalyst to compare the classic APTES and amine-epoxy methods with the bis-amino silane. None of the formulations with 100% water as a solvent produced stable bonds in DMEM after two weeks. In addition, the bis-amino formulation for treatment 2 was unstable and rapidly polymerized. The instability can be explained by the difference in number of alkoxy silane groups per molecule of silane. Compared to APTES, the bis-amino silane has twice the number of reactive groups and a flexible C₃H₆-NH-C₃H₆ chain that promotes crosslinking. While hydrolysis of the alkoxy silane to Si-OH must occur before the condensation of a silane molecule on the PET surface, too many hydrolyzed Si-OH groups can result in polymerization or precipitation for a dipodal silane. Similarly, too much water present can inhibit the growth

of the silane layer by hydrolysing the C-O-Si bonds before the silane molecules and the substrate can generate a stable surface coating. Therefore, we assayed solution stability for the bis-amino silane and APTES in different concentrations of water and isopropyl alcohol (IPA). We found that solutions of 2% bis-amino silane were stable in IPA with up to 1% water. Greater concentrations resulted in bulk gelation or precipitation. 2% APTES solutions were stable at all concentrations of water and IPA tested.

For treatments 4–9, we compared 1% water, 0.5% titanate catalyst (TBT), and no catalyst with either 2% APTES or 2% bis-amino silane. None of the APTES treated samples remained bonded after 1 day of immersion in DMEM at 37 °C. For the bis-amino formulations, there was partial bonding of the samples for the TBT catalyzed or un-catalyzed formulations after two weeks. Full bonding was realized after two weeks in DMEM for treatment 5 with 2% bis-amino silane in 1% water and IPA. Interestingly, treatment 10 also realized full bonding through an amine-epoxy bonding mechanism, in which the PET membrane was treated with a solution 2% APTES and 0.5% TBT in IPA and the PDMS sample that was treated with 2% epoxy-silane and 0.5% TBT in IPA. Upon comparison to treatment 3, in which 100% water was used in order to replicate amine-epoxy bonding as reported in the literature, the result of treatment 10 suggests that the amount and type of catalyst used is critical for the silane modification process. While 100% water-based silane treatments may work well for PDMS or glass substrates, the lower concentration of hydroxyl groups on an oxidized PET surface could limit the condensation and surface coverage of the silane coating. The amine-epoxy method was not improved by the addition of bis-amino silane to promote cross-linking, as demonstrated by the bond failures after two weeks for treatment 11.

XPS analysis of surface composition of silane modified PET and degradation of silane layer

The chemical composition of the untreated, oxygen plasma treated, and silane modified PET membranes were determined using XPS analysis shown in Fig. 2(a). The atomic concentration of the untreated PET samples was measured to be 75.4% C and 24.4% O with negligible Si or N content. The oxygen plasma treatment resulted in an increase to 30.3% O with 2% N and 0.5% Si. The slight presence of Si can be attributed to PDMS contamination from within the plasma oven chamber. Notably, samples treated with bis-amino silane resulted in greater than twofold increase in the concentrations of silicon and nitrogen when compared to the

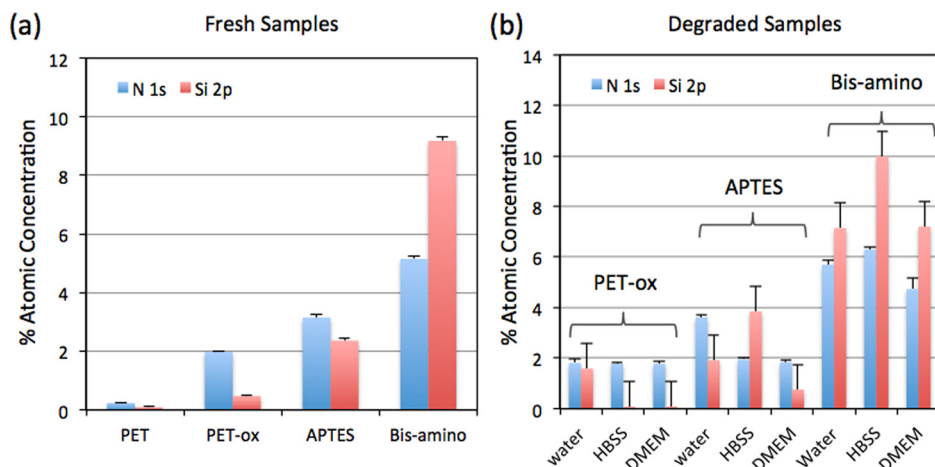


FIG. 2. XPS elemental composition analysis for silane treated PET membrane samples. (a) Comparison of the nitrogen and silicon atomic concentration derived from XPS analysis of untreated PET track-etched membranes, oxygen plasma treated (PET-ox), APTES treated, and bis-amino treated samples. (b) Comparison of nitrogen and silicon atomic concentration of oxygen plasma treated, APTES, and bis-amino silane treated membranes after degradation by immersion in water, HBSS, or DMEM for 18.5 h. Error bars indicate the standard deviation.

APTES treatment (Fig. 2(a)). The effects of different aqueous solutions on the degradation of silane treatments was analysed by measuring the chemical composition with XPS after 18.5 h of immersion at 37°C. The results in Fig. 2(b) show that while APTES loses silicon and nitrogen after exposure to DMEM, bis-amino silane treated samples remain relatively unchanged. Example of XPS spectra and full elemental composition data is included in the supplementary material²⁹ in Fig. S1 and Tables S1 and S2.

Demonstration of long-term culture and basal-side stimulation of differentiated myotubes

The optimal treatment of PET membranes with 2% bis-amino silane in 1% water and IPA was used to fabricate an open-surface device for long-term cell culture. We used a simple microfluidic design for the basal-side stimulation of cell cultures as shown in Fig. 3. C2C12 myoblasts were chosen as a representative cell type to demonstrate compatibility of the method with substrate coating, differentiation, long-term culture of adherent cells, and functional testing of membrane-based reagent delivery. C2C12 cells were seeded at low density onto the PET membrane surface and allowed to propagate to confluence for one week. The cells were differentiated into myotubes by culturing in differentiating medium for an additional week. To demonstrate stable bonding and functionality of the track-etched pores, we operated the device by loading a calcein-AM solution into the microfluidic channel. Cells grown above the microchannels were locally stained as shown in Figs. 3(c)–3(e).

Rapid delamination is predicted for devices with a porous surface in contact with medium

In our testing, we have investigated bonding to open-surface devices, in which one surface of the porous membrane is entirely exposed to the surrounding medium during immersion. Initially, we were surprised to find that the existing methods using APTES^{20,30} or amine-epoxy bonding²⁴ resulted in rapid delamination after immersion in DMEM for one day at 37°C (see

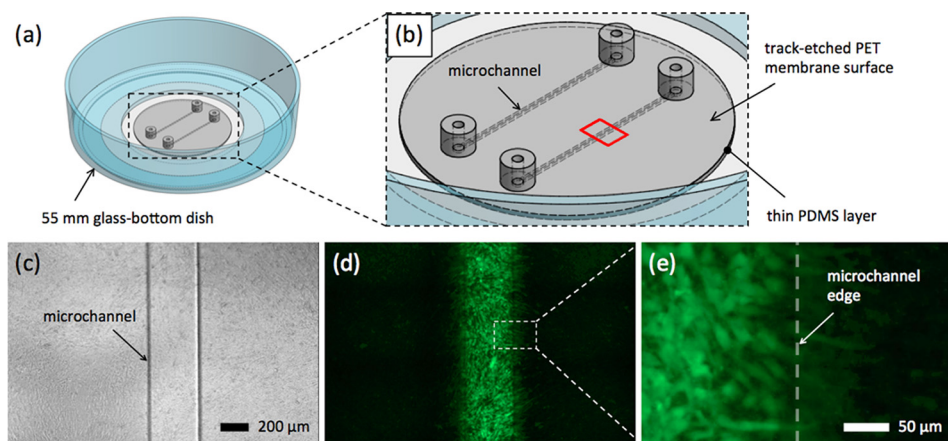


FIG. 3. Demonstration of bis-amino silane bonding for cell culture compatibility and long-term stability. (a) An isometric schematic is shown for an open-surface basal-side stimulation device. The device is integrated into a cover-glass bottom 55 mm dish to accommodate standard cell culture practice. (b) A track-etched PET membrane comprises the cell culture substrate and seals the underlying PDMS microchannels. The red outlined box indicates the field of view for the microscopy images in (c)–(e). (c) A phase contrast image of differentiated C2C12 myotubes grown on a Matrigel coated surface of the device after 2 weeks in culture. (d) A fluorescent image showing the targeted basal-side delivery of calcein-AM to a region of the cell layer adjacent to the microfluidic channel. (e) A close-up view shows individual myotubes and highlights the diffusion of calcein-AM at the microchannel edge. Intracellular calcein-AM detection is limited to cells located between 50–100 μm away from the microchannel. This indicates that the bond interface is intact and that the dye is only able to escape from the microchannel-pore interface. In contrast, bond failure would result in catastrophic leakage of the dye and wide staining of the cell culture surface (data not shown).

Table I). In order to explain the difference between our results and those previously reported in the literature, we present an analysis of the open surface geometry and the silane layer delamination rate.

A porous membrane has a much higher perimeter available for hydrolytic attack when only one side is sealed with PDMS. Each individual pore presents an interface at which the surrounding medium can begin hydrolysis of the interfacial silane layer. For example, a membrane sandwiched between two PDMS slabs of 4 mm in radius has a perimeter of 25.1 mm (Fig. 4(a)). For a membrane bonded on only one side in an open-surface configuration (Fig. 4(b)) the effective perimeter can be expressed by

$$P = \varepsilon A_0 \pi 2r + \pi 2R, \quad (1)$$

where ε is the porosity, A_0 is the area of the membrane, r is the radius of a single pore, and R is the radius of the slab. For a porosity of 2×10^{10} pores m^{-2} and a pore diameter of $0.4 \mu\text{m}$, the effective perimeter is approximately 1.28 m due to the large contribution of the exposed pores. This amounts to a nearly 50-fold difference in the perimeter available for hydrolytic degradation. Now, if we also account for the increase in the pore size as a result of delamination, Eq. (1) becomes

$$P = \varepsilon A_0 \pi 2(r + \Delta) + \pi(d - 2\Delta), \quad (2)$$

where Δ is the delamination radius for a given unit of time as shown in Figs. 4(c) and 4(d). Similarly, we can describe the area of delamination as a function of time for a sandwiched sample configuration using the expression

$$A(t) = A_0 - \pi[R - r(t)]^2, \quad (3)$$

where $r(t)$ is the delamination radius as a function of time. For the open-surface configuration, we must account for the area of delamination contributed by each individual pore with the expression

$$A_{open}(t) = \varepsilon A_0 \pi[r + r(t)]^2 - \varepsilon A_0 \pi r^2 + A(t). \quad (4)$$

Therefore, the area of delamination for each condition is expressed by a quadratic function of $r(t)$. Comparing the coefficients for $r(t)^2$ for the open-surface and sandwiched configuration, we have

$$\varepsilon A_0 \pi \text{ vs. } \pi. \quad (5)$$

The product of εA_0 is the total number of pores for the surface area of the bonded sample; therefore, the rate of delamination depends heavily on the porosity of the membrane used in

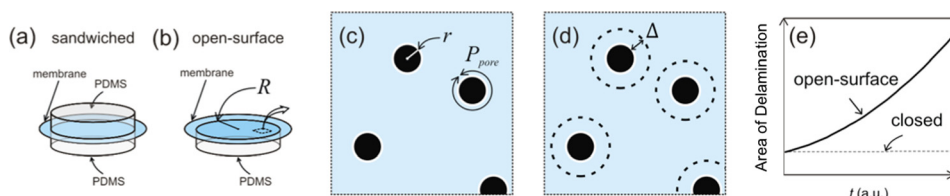


FIG. 4. Geometric considerations for bond delamination of track-etched membranes. (a) In a sandwiched configuration, both sides of the membrane are bonded to PDMS slabs. In this configuration, the perimeter available to hydrolytic attack is determined by the radius of the sample. (b) In an open-surface configuration, the membrane is bonded to only one side of a PDMS slab while exposing a large porous surface area to the medium. (c) A schematic of the surface of the membrane depicts the pore radius and perimeter. Each individual pore contributes to the total perimeter available for hydrolytic attack and delamination of the bond interface. (d) During delamination as the radius increases, the effective perimeter in contact with the medium grows to accelerate the process. (e) Plotting the theoretical area of delamination for an arbitrary growth rate as in Eq. (5) predicts that the open-surface configuration would decay 1.0×10^6 times faster than a closed configuration under the same conditions. Samples were tested using the open-surface configuration in order to determine an effective silane bonding strategy for the more challenging configuration.

our sample. For a comparison between the delamination of open-surface and sandwiched samples, see Fig. 4(e). This analysis predicts a rate of delamination that is $\varepsilon A_0 = 1.0 \times 10^6$ times faster for an open-surface sample compared to a sandwiched sample. This rapid degradation at first appears to be a fundamental limitation of the method; however, individual bonds can re-associate under equilibrium. In theory, the strength of a silane interfacial layer is due to the number of bonds and the continual reorganization of the bonds to minimize the stress at the interface between the two substrates.²¹ However, with the contamination of this interface by cations from the medium, the equilibrium process could be disrupted to favour hydrolysis of the layer. The cation induced hydrolysis can explain the difference in stability of sandwiched and open-surface samples bonded using APTES. Our solution is to employ a dipodal silane in which the individual silane molecule has 6 alkoxy silane functional groups available for bonding. Studies have shown that dipodal silanes are more effective anti-corrosion treatments for metals exposed to harsh salt solutions.³¹ According to a leading manufacturer of silanes, Gelest, Inc., the use of a dipodal silane can theoretically improve bond strength by 100 000 times at equilibrium since the number of bonds increases from three to six per silane molecule.²⁶ We believe the theoretical bond strength of the dipodal silanes imparts substantial improvement to the process and ultimately negates the effects of the corrosive medium and the open-surface geometry.

CONCLUSIONS

We initially observed rapid delamination of open-surface devices fabricated using APTES bonding methods when immersed in DMEM. Our theoretical analysis of the rate of delamination offers an explanation to the mechanism of this observed increase in the rate of degradation. Following the assay of a variety of silane formulations, we determined that the 2% bis-amino silane in 1% water and IPA offered the most straightforward method for producing stably bonded open-surface devices. Using XPS analysis, we confirmed changes in the elemental composition for silane-treated membranes and found that bis-amino silane results in greater and more stable introduction of silicon and nitrogen than APTES. We demonstrated the long-term bond stability of this silane treatment with the operation of a simple device for the basal-side stimulation of differentiated C2C12 myotubes. Our study was focused on PDMS based devices because it has excellent optical clarity and elastomeric properties. For bonding to thermoset polymers like track-etched membranes, PDMS is advantageous because it can accommodate surface roughness through elastomeric deformation. To extend our method for sensitive bioanalytical assays there exist compatible techniques to reduce the adsorption of biomolecules into PDMS with coatings such as Parylene C.^{32,33} Although we focused on PET, track-etched membranes are also commonly available in polycarbonate (PC). PC can also be effectively modified with O₂ plasma, so we speculate that our method would be compatible. We believe the methods presented here are valuable to the future development of novel PDMS microfluidic devices based on the integration of porous membranes for applications such as gradient assays, co-cultures, and organs-on-chips.

ACKNOWLEDGMENTS

Support for this work was generously provided by the NIH/NIBIB (Grant No. R01 EB007526).

¹Y. Torisawa, B. Chueh, D. Huh, P. Ramamurthy, T. M. Roth, K. F. Barald, and S. Takayama, "Efficient formation of uniform-sized embryoid bodies using a compartmentalized microchannel device," *Lab Chip* **7**(6), 770–776 (2007).

²T. Kim, M. Pinelis, and M. M. Maharbiz, "Generating steep, shear-free gradients of small molecules for cell culture," *Biomed. Microdevices* **11**(1), 65–73 (2009).

³D. M. Cate, C. G. Sip, and A. Folch, "A microfluidic platform for generation of sharp gradients in open-access culture," *Biomicrofluidics* **4**(4), 044105 (2010).

⁴V. V. Abhyankar, M. A. Lokuta, A. Huttunen, and D. J. Beebe, "Characterization of a membrane-based gradient generator for use in cell-signaling studies," *Lab Chip* **6**(3), 389 (2006).

⁵C. G. Sip, N. Bhattacharjee, and A. Folch, "Microfluidic transwell inserts for generation of tissue culture-friendly gradients in well plates," *Lab Chip* **14**(2), 302–314 (2014).

⁶J. Kawada, H. Kimura, H. Akutsu, Y. Sakai, and T. Fujii, "Spatiotemporally controlled delivery of soluble factors for stem cell differentiation," *Lab Chip* **12**(21), 4508–4515 (2012).

⁷C. Kim, K. Kreppenhofer, J. Kashef, D. Gradl, D. Herrmann, M. Schneider, R. Ahrens, A. Guber, and D. Wedlich, "Diffusion- and convection-based activation of Wnt/β-catenin signaling in a gradient generating microfluidic chip," *Lab Chip* **12**(24), 5186–5194 (2012).

⁸A. A. Epshteyn, S. Maher, A. J. Taylor, A. B. Holton, J. T. Borenstein, and J. D. Cuffi, "Membrane-integrated microfluidic device for high-resolution live cell imaging," *Biomicrofluidics* **5**(4), 046501 (2011).

⁹A. K. H. Achyuta, A. J. Conway, R. B. Crouse, E. C. Bannister, R. N. Lee, C. P. Katnik, A. A. Behensky, J. Cuevas, and S. S. Sundaram, "A modular approach to create a neurovascular unit-on-a-chip," *Lab Chip* **13**(4), 542–553 (2013).

¹⁰D. Huh, B. D. Matthews, A. Mammoto, M. Montoya-Zavala, H. Y. Hsin, and D. E. Ingber, "Reconstituting organ-level lung functions on a chip," *Science* **328**(5986), 1662–1668 (2010).

¹¹R. F. Ismagilov, J. M. K. Ng, P. J. A. Kenis, and G. M. Whitesides, "Microfluidic arrays of fluid–fluid diffusional contacts as detection elements and combinatorial tools," *Anal. Chem.* **73**(21), 5207–5213 (2001).

¹²T.-C. Kuo, D. M. Cannon, Y. Chen, J. J. Tulock, M. A. Shannon, J. V. Sweedler, and P. W. Bohn, "Gateable nanofluidic interconnects for multilayered microfluidic separation systems," *Anal. Chem.* **75**(8), 1861–1867 (2003).

¹³Y. Zhang and A. T. Timperman, "Integration of nanocapillary arrays into microfluidic devices for use as analyte concentrators," *Analyst* **128**(6), 537–542 (2003).

¹⁴B. R. Flachsbart, K. Wong, J. M. Iannaccone, E. N. Abante, R. L. Vlach, P. A. Rauchfuss, P. W. Bohn, J. V. Sweedler, and M. A. Shannon, "Design and fabrication of multilayered polymer microfluidic chip with nanofluidic interconnects via adhesive contact printing," *Lab Chip* **6**(5), 667–674 (2006).

¹⁵S. N. Masand, L. Mignone, J. D. Zahn, and D. I. Shreiber, "Nanoporous membrane-sealed microfluidic devices for improved cell viability," *Biomed. Microdevices* **13**(6), 955–961 (2011).

¹⁶M. Morel, J.-C. Galas, M. Dahan, and V. Studer, "Concentration landscape generators for shear free dynamic chemical stimulation," *Lab Chip* **12**(7), 1340 (2012).

¹⁷B. Chueh, D. Huh, C. R. Kyrtos, T. Houssin, N. Futai, and S. Takayama, "Leakage-free bonding of porous membranes into layered microfluidic array systems," *Anal. Chem.* **79**(9), 3504–3508 (2007).

¹⁸J. J. VanDersarl, A. M. Xu, and N. A. Melosh, "Rapid spatial and temporal controlled signal delivery over large cell culture areas," *Lab Chip* **11**(18), 3057 (2011).

¹⁹H. Kimura, T. Yamamoto, H. Sakai, Y. Sakai, and T. Fujii, "An integrated microfluidic system for long-term perfusion culture and on-line monitoring of intestinal tissue models," *Lab Chip* **8**(5), 741–746 (2008).

²⁰K. Aran, L. A. Sasso, N. Kamdar, and J. D. Zahn, "Irreversible, direct bonding of nanoporous polymer membranes to PDMS or glass microdevices," *Lab Chip* **10**(5), 548 (2010).

²¹E. P. Plueddemann, *Silane Coupling Agents* (Springer, 1982).

²²M. E. Vlachopoulou, A. Tserepi, P. Pavli, P. Argitis, M. Sanopoulou, and K. A. Misiakos, "A low temperature surface modification assisted method for bonding plastic substrates," *J. Micromech. Microeng.* **19**, 015007 (2009).

²³Z. Zhang, P. Zhao, and G. Xiao, "The fabrication of polymer microfluidic devices using a solid-to-solid interfacial poly-addition," *Polymer* **50**(23), 5358–5361 (2009).

²⁴L. Tang and N. Y. Lee, "A facile route for irreversible bonding of plastic-PDMS hybrid microdevices at room temperature," *Lab Chip* **10**(10), 1274 (2010).

²⁵K. S. Lee and R. J. Ram, "Plastic–PDMS bonding for high pressure hydrolytically stable active microfluidics," *Lab Chip* **9**(11), 1618 (2009).

²⁶See <http://www.gelest.com/goods/pdf/faq/question%208.pdf> for Gelest, Inc., Difficult Substrates.

²⁷C.-H. Hsu, C. Chen, and A. Folch, "Microcanals for micropipette access to single cells in microfluidic environments," *Lab Chip* **4**(5), 420 (2004).

²⁸D. Yaffe and O. Saxel, "Serial passaging and differentiation of myogenic cells isolated from dystrophic mouse muscle," *Nature* **270**(5639), 725–727 (1977).

²⁹See supplementary material at <http://dx.doi.org/10.1063/1.4883075> for example XPS spectra and elemental composition data.

³⁰V. Sunkara, D.-K. Park, H. Hwang, R. Chantiwas, S. A. Soper, and Y.-K. Cho, "Simple room temperature bonding of thermoplastics and poly(dimethylsiloxane)," *Lab Chip* **11**(5), 962 (2011).

³¹D. Zhu and W. J. van Ooij, "Enhanced corrosion resistance of AA 2024-T3 and hot-dip galvanized steel using a mixture of bis-[triethoxysilylpropyl]tetrasulfide and bis-[trimethoxysilylpropyl]amine," *Electrochim. Acta* **49**(7), 1113–1125 (2004).

³²Y. S. Shin, K. Cho, S. H. Lim, S. Chung, S.-J. Park, C. Chung, D.-C. Han, and J. K. Chang, "PDMS-based micro PCR chip with Parylene coating," *J. Micromech. Microeng.* **13**(5), 768 (2003).

³³T. Y. Chang, V. G. Yadav, S. De Leo, A. Mohedas, B. Rajalingam, C.-L. Chen, S. Selvarasah, M. R. Dokmeci, and A. Khademhosseini, "Cell and protein compatibility of parylene-C surfaces," *Langmuir* **23**(23), 11718–11725 (2007).